Journal of the European Ceramic Society 20 (2000) 127–132

# Characterization of plasma sprayed nano-titania coatings by impedance spectroscopy

Yingchun Zhu*, Chuanxian Ding

*Shanghai Institute of Ceramics, Chinese Academy of Sciences, Shanghai, 200050, People's Republic of China*

Received 11 December 1998; received in revised form 6 April 1999; accepted 11 May 1999

**Abstract**

Nano-titania coatings were deposited via vacuum plasma spraying. The microstructure and chemical state of the coatings were investigated with SEM, TEM, XRD and XPS, respectively. The results showed that the vacuum plasma sprayed titanium oxide coatings possessed porous structure with small pores and agglomerated nanosized grains. The ac electrical data were measured in the frequency range $1 \leqslant f \leqslant 10^7$ Hz at room temperature. The electrical data were analyzed with complex resistance and complex capacitance plots. The terminal resistance and capacitance were dissected with relation to the structure of the coatings. The depression observed in the planes was analysed in terms of nonuniformity in the measured reactance between the terminals. 

*Keywords:* Coatings; Electrical properties; Impedance spectroscopy; Plasma spraying; $TiO_2$

## 1. Introduction

Metal oxides, such as $SnO_2$, ZnO, $Fe_2O_3$, $TiO_2$, $WO_3$ and $ZrO_2$, has been extensively used as humidity sensors and gas sensors to detect CO, $H_2$, $O_2$, $NO_X$, $NH_3$ and $SO_2$.[1–5] Recently, nanostructured semiconducting oxides have been prepared and applied to gas sensors and exhibited high quality because of their small grain size, large surface and special structure.[6–8] Dong et al. prepared nano ZnO, ZnO–Fe, ZnO–Ag, etc., and studied their gas sensing properties. It was reported that the sensitivity of nano ZnO was improved and the operating temperatures were lowered due to the nanostructure of oxides.[7]. Lin et al. processed nano $TiO_2$ and $Pt/TiO_2$ and investigated their gas sensing properties and found that the optimal operation temperature for $NO_2$ and CO gas was 190°C for the nano $TiO_2$ sensor and 170°C for the nano $Pt/TiO_2$ sensor.[8]

In the present work, nano $TiO_2$ coatings were prepared with vacuum plasma spray and their electrical properties were investigated using impedance spectroscopy. Vacuum plasma spraying (VPS) of nanostructured coatings is a new process comparing with other methods.[9] It has been found that the plasma sprayed nano-$TiO_2$ coatings possessed a porous structure, which maybe have unique characters as sensing materials. The electrical property of sensors is influenced with microstructure of sensing materials, i.e. the grain and grain boundary as well as complex-phase structure.[10] Impedance spectroscopy is an effective technique to characterize the electrical nature of heterogeneous composite systems. The intergranular electrical barriers, origin of resistance or capacitance, their dispersion with a small-signal frequency and the role of defects in the electric field can be ascertained with Impedance spectroscopy. This paper reports the microstructure of the $TiO_2$ coatings prepared by VPS, and the microstructure–property relationship of the sensing material according to the Impedance spectroscopy.

## 2. Experimental procedure

Spray powders were synthesized through controlled hydrolysis of titanium butoxide in an ethanol aqueous solution. The process of manufacturing spray powders can be briefly described as follows: hydrolysis of titanium butoxide, direct precipitation and drying at 60–70°C under a pressure of $3\times10^4$ Pa for 2 h. The powders are aggregates of spherical or ellipsoidal morphology with a size ranging from 50 to 100 nm in diameter with

* Corresponding author.
*E-mail address:* cxding@sunm.shcnc.ac.cn (Y. Zhu).

0955-2219/00/$ - see front matter 
PII: S0955-2219(99)00159-4

an anatase phase. The details of the powder preparation were described elsewhere.[11]

A-2000 vacuum plasma spraying equipment (Sulzer Metco AG, Switzerland) was used to deposit nano titanium oxide coatings. The powders were fed with a Twin-System 10-V (Plasma-Technik AG, Switzerland). The plasma spraying process was carried out in an Ar gas atmosphere under a pressure of 30 mbar. The plasma parameters are as follows: plasma power is 13.6 kVA, depositing distance is 270 mm, plasma forming gas is 70 slpm for coating (A) and 35 slpm for coating (B), respectively. The coatings were deposited on Quartz glass plate and forked electrode respectively for different measurements.

The surface morphology of the coatings was determined with an EPMA-8705QH22 (Shimadzu, Tokyo, Japan) Electron Probe Analyzer. The coatings were scraped from the substrates and analyzed with a JEM-200CX (Jeol, Tokyo, Japan) Transmission Electron Microscope (TEM). The crystal structure of the coatings was measured with an RAX-10 (Rigaku, Tokyo, Japan) X-ray Diffractometer (XRD). X-ray photoelectron spectroscopy analyses (XPS) was also carried out to examine the chemical state of titanium oxide coatings with a PHI 5000C ESCE System (Perkin–Elmer, USA). The impedance spectroscopy was measured on a SI 1260 Impedance/Gain-Phase Analyzer (Schlumberger) in the frequency ranging from 1 to $10^7$ Hz at room temperature in air. The acquired data are known as complex impedance ($Z^*$) and complex capacitance ($C^*$), and there are following relationships: $Z^* = 1/iwC^*$, $Z^* = Z' + iZ''$ and $C^* = C' + iC''$.

## 3. Results and discussion

### 3.1. Microstructure of nanostructured titanium oxide coatings

The surface morphologies of vacuum plasma sprayed titanium oxide coatings are presented in Fig. 1. From Fig. 1, it can be seen that the as-prepared titanium oxide coatings possess a porous structure composed of small pores and grains. Fig. 2 showed the TEM micrographs of nanostructured titanium oxide coatings. From Fig. 2 it can be found that the grains observed in SEM micrographs are composed of ultra-fine grains with particle size ranging from 10 to 100 nm and micro pores among the nanosized grains. Both coatings possess nanophase structure. Comparing the microstructure of the two coatings, it can be found that coating (B) is more densely compacted than coating (A).

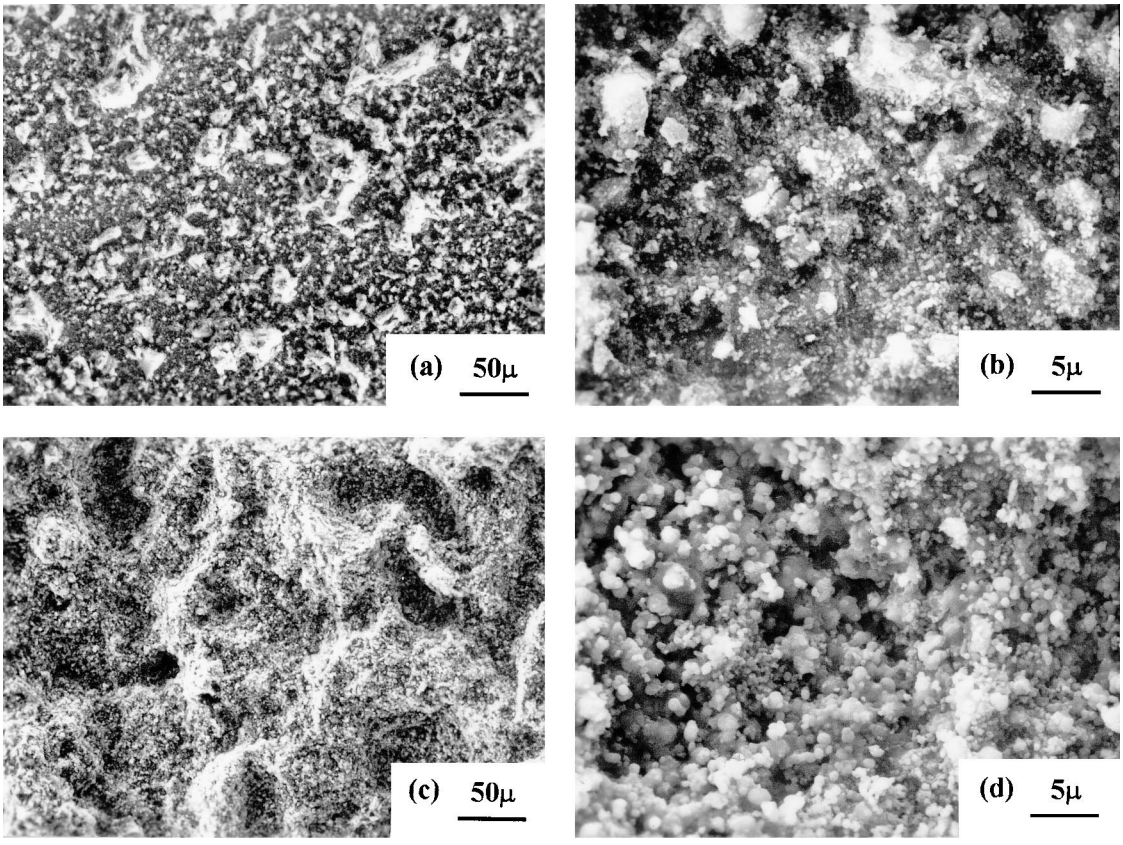


Fig. 1. SEM morphologies of plasma sprayed titanium oxide coatings: (a) and (b): coating (A); (c) and (d): coating (B).

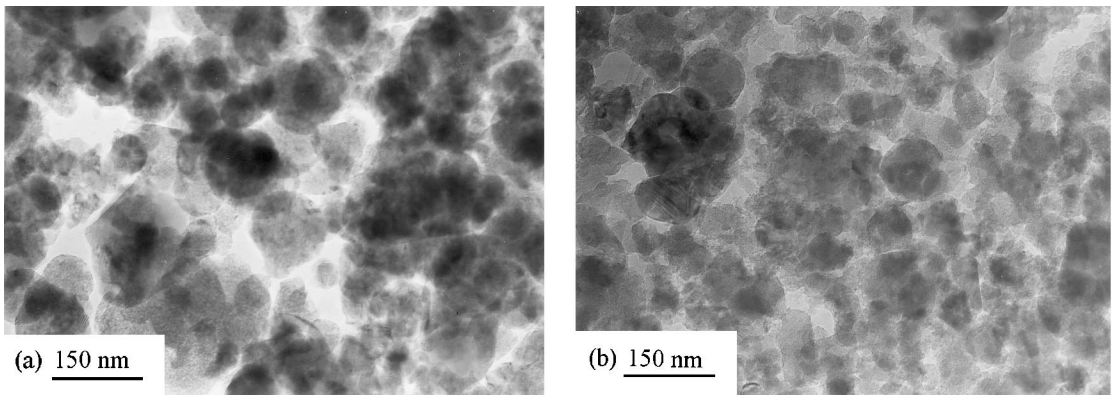


Fig. 2. TEM morphologies of plasma sprayed titanium oxide coatings: (a): coating (A), (b): coating (B).

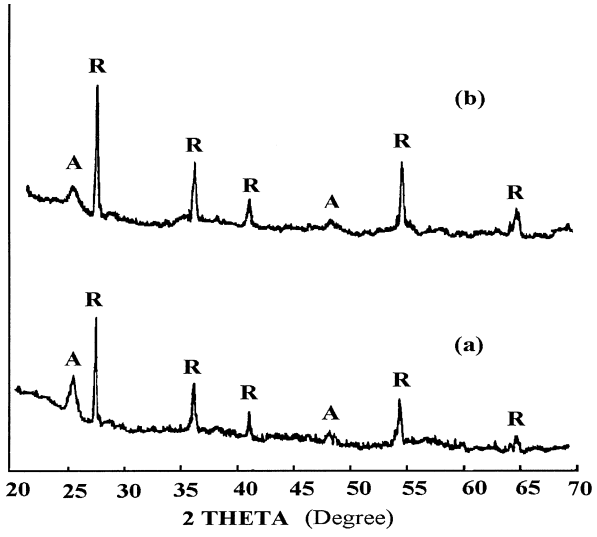


Fig. 3. XRD patterns of plasma sprayed titanium oxide coatings: (a): coating (A); (b): coating (B).

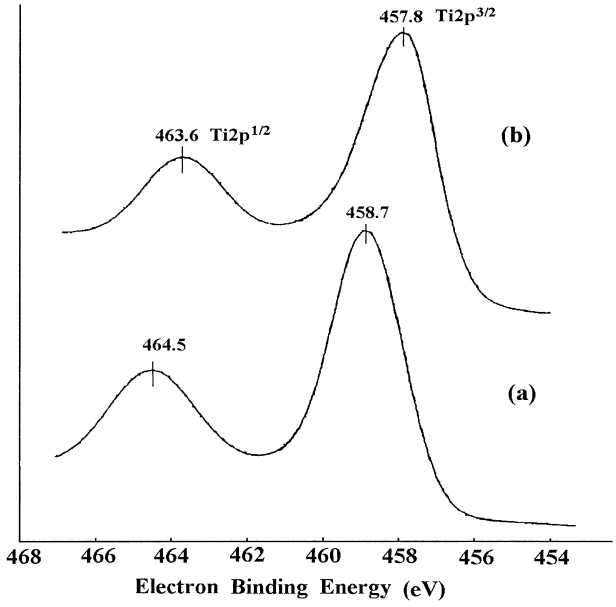


Fig. 4. XPS spectra of plasma sprayed titanium oxide coatings: (a): coating (A); (b): coating (B).

### 3.2. XRD analyses of nano $TiO_2$ coatings

X-ray diffraction patterns of the as-prepared coatings are presented in Fig. 3. Both coatings have similar X-ray diffraction patterns and are composed of rutile and anatase phase.[12] From the intensity of diffraction peaks, it can be found that the two coatings are mainly composed of rutile phase with a little of anatase phase. Comparing the relative diffraction intensity of anatase and rutile in coating (A) and (B), it is indicated that coating (A) contains more anatase than coating (B).

### 3.3. X-ray photoelectron spectroscopy analyses

Fig. 4 showed XPS spectra of the nano titanium oxide coatings. The binding energies of Ti ($2p^{1/2}$) and Ti ($2p^{3/2}$) of coating (A) are 464.5 and 458.7 eV, which corresponds with those of titania.[13] The binding energies of Ti ($2p^{1/2}$) and Ti ($2p^{3/2}$) of coating (B) are 463.6 and 457.8 eV, which is lower than those of titania.[13] The results revealed that there were low-valence titanium cations in titanium oxide coating (B). The formation of low-valence titanium cations resulted from the deoxidization of $TiO_2$ powders owing to the high temperature and low pressure during the plasma spraying process.

The foregoing results showed that both coating (A) and coating (B) possessed porous nanophase structure and were mainly composed of rutile phase with a little of anatase phase. Vacuum plasma spraying is a rapid process, the residence time of $TiO_2$ powders inside the plasma jet is too short for nano-$TiO_2$ powders to grow up.[14] Thus, the particles in the films remain nanostructured. Although the residence time of $TiO_2$ powders inside the plasma jet is very short, the temperature of plasma jet is as high as 15000°C,[15] the high temperature changed the crystallinity of titania powder. The temperature of plasma jet changes dramatically from the

centre to the outside, and titania powders were injected into different positions of plasma jet. Thus, the amorphous titania powders were transferred into a mixture of anatase and rutile phase. The high temperature also led to the decomposition and evaporation of nanostructured titania powders and thus led to a porous coating.

The differences in the structure of coating (A) and coating (B) were introduced by the different plasma parameters. The plasma flow rate of coating (B) is lower than that of coating (A). With the decrease of plasma flow rate, the temperature of plasma jet goes up, the plasma jet velocity is reduced, the residence time of the particles inside the plasma jet increases, and the melting state of powders is improved. Thus, coating (B) is dense, contains more rutile and low-valence titanium cations comparing with coating (A).

### 3.4. Impedance spectroscopy analyses

The polycrystalline structure and the corresponding equivalent circuit of nano titanium oxide sensor are illustrated in Fig. 5. $R_0$ is the electrical contact resistance; $R_1$, $C_1$ and $R_2$, $C_2$ are the resistance and capacitance of grain boundary and grain body, respectively.

The impedance plot of titanium oxide coating (A) is presented in Fig. 6. The impedance plot shows depressed overlapping semicircle, which is the lumped response of the grain and grain boundary contributions between the terminals. The left high frequency part of the semicircle corresponds to the response of grain body, while the low frequency part corresponds to the response of grain boundary. The overlapped semicircle indicates that the distinct relaxation time ($\tau_1/\tau_2'$ is less than 100, wherein $\tau_1$ for grain and $\tau_2$ for grain boundary. The left high frequency part of the semicircle corresponds to the response of grain body, while the low frequency part corresponds to the response of grain boundary. The $Z^*$-plane of titanium oxide coating (B) presented in Fig. 7 also shows overlapping semicircle. However, the left high frequencies part in the $Z^*$-plane of coating (B) corresponding to the grain body is almost not depressed.

The depression of the semicircles in the $Z^*$-plane was attributed to nonuniformity in the defect levels from one junction to another; nonuniformity in the defect levels within each junction; or a combination of these two processes.[6] Coating (A) possesses a looser structure as shown in Figs 1 and 2(a), in addition, coating (A) contains more anatase than coating (B) presented in Fig. 3. Therefore, the uniformity of coating (A) is lower than that of coating (B), which may be the reason why the first semicircle in the $Z^*$-plane of coating (A) is depressed but that of coating (B) is not. Conversely, the

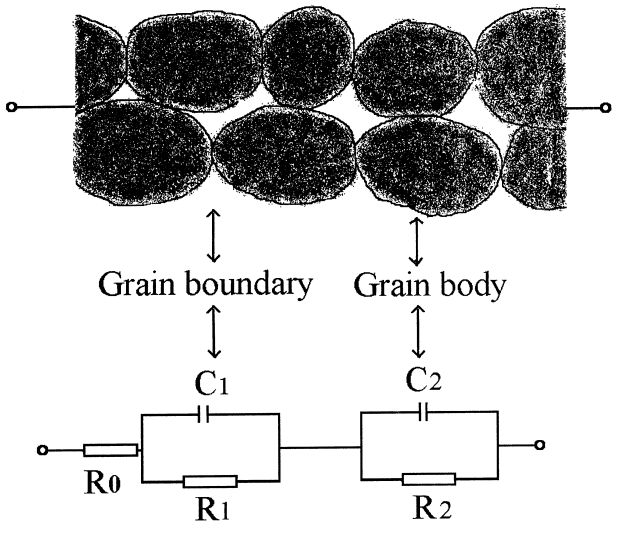


Fig. 5. The diagram of microstructure and equivalent circuit of nano titanium oxide sensor.

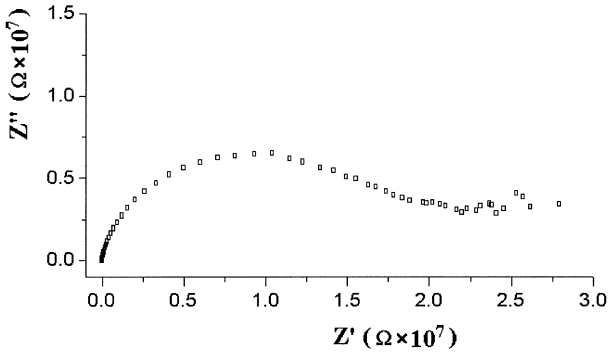


Fig. 6. Impedance plot of plasma sprayed titanium oxide coating (A).

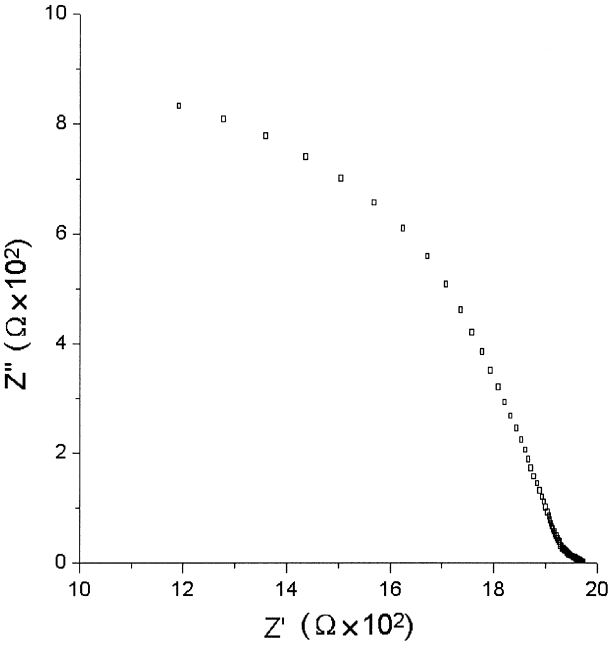


Fig. 7. Impedance plot of plasma sprayed titanium oxide coating (B).

depression of the semicircle in the $Z^*$-plane of coating (A) shows that the uniformity of coating (A) is lower than that of coating (B).

Comparing the $Z^*$-planes of coatings (A) and (B), it can also be found that coating (A) possesses a higher resistance than coating (B). This can be attributed to the differences in their microstructure as the foregoing discussion. Dense coating should have low resistance. Particularly, the presence of low-valence titanium shown in Fig. 4 is an important factor influencing on the resistance of coating (B). Low concentration of electron or hole could greatly improve the conductivity of semiconductors.[16] The low-valence titanium acts as a donor in the semiconducting titania coating and therefore improves the conductivity of the coating.

The complex capacitance of coating (A) and (B) is presented in Figs. 8 and 9, respectively. The two $C^*$-planes have similar patterns: the intercept capacitance on the real axis at high frequencies; the overlapping semicircle at high frequencies; and the distorted semicircle at low frequencies. The intercept capacitance at high frequencies originates from the barrier layer effect of the grain boundary and the single-crystal-like behaviour of the grain, and the barrier layer capacitance is mainly dominated by the trap-free electrical thickness across the grain boundary.[17,18] The two overlapping semicircles at high and low frequencies arise from defects formed at the grain boundaries, which serves as trapping levels within the electrical thickness of grain boundary.

Comparing the $C^*$-planes in Figs. 8 and 9, it can be found that the intercept of the capacitance of coating (B) is apparently larger than that of coating (A), which is associated with their microstructures. As foregoing observed and discussed, coating (B) is more densely compacted with reduction of its porosity. The densely compacted structure results in the reduction of electrically active junctions and the grain boundary electrical thickness, hence increases the barrier layer capacitance. Additionally, the low-valence titanium presented in coating (B) enhanced the barrier layer polarization and improved the permittivity of titania coating, thus increase the capacitance.

Azad et al. sintered titania samples and studied their electrical property using immittance spectroscopy.[6] Comparing to the result of Azad, the semicircle in the $Z^*$-plane of plasma sprayed nano-titania coatings is more apparent; the dc resistance is smaller and can be changed dramatically in the range from $2.5\times10^7$ to $2\times10^3$ Ω. The appearance of capacitance plot of plasma sprayed titania coating is similar to that of sintered titania samples, despite the fact that the capacitance of plasma sprayed nano-titania coatings is larger than that of the sintered titania sample. The differences in the immittance spectroscopy of sintered and plasma sprayed samples are related to their different structures. The plasma sprayed titania coatings are a mixture of anatase and rutile phase, while the sintered samples contains only anatase or rutile phase. Two-phase mixture could reduce the resistance of samples because of the interface effect.[6,19] As foregoing discussion, the low-valance titanium cations in the plasma sprayed titania coating is an important factor influencing the resistance of the plasma nano-titania coating. TEM analyses showed that plasma sprayed nano-titania coatings are

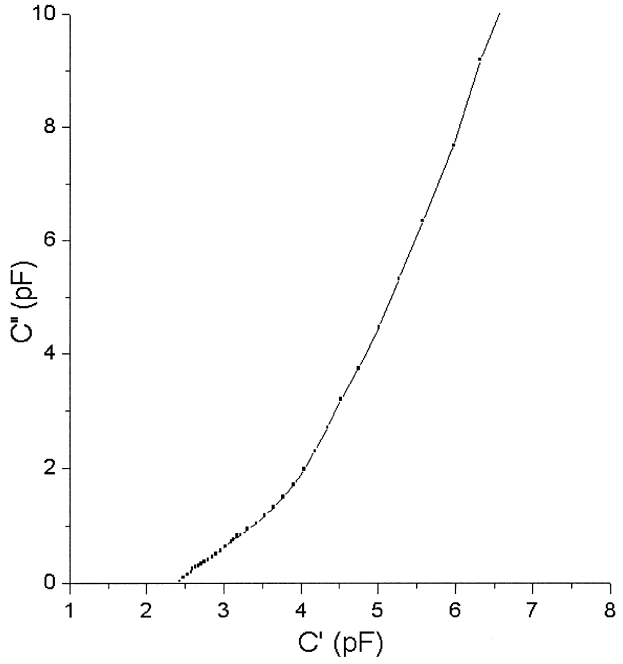


Fig. 8. Capacitance plot of plasma sprayed titanium oxide coating (A).

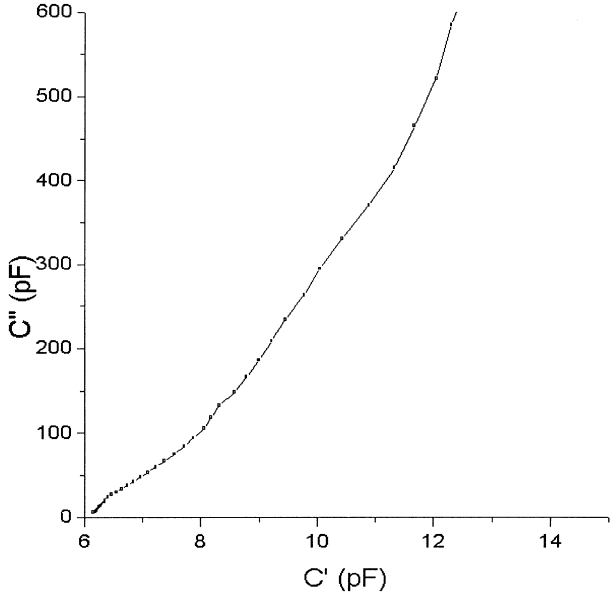


Fig. 9. Capacitance plot of plasma sprayed titanium oxide coating (B).

composed of ultra-fine particles which lead to a great deal of intergranular component. The intergranular component improved the electric conductivity of titania coatings.[20]

Plasma sprayed titania coatings possess nanophase structure and a great deal of intergranular component. Impedance spectroscopy analyses showed that the nanophase and interface structure of the plasma sprayed coatings greatly changed the electric property of titania. As a sensing material, plasma sprayed nano-titania coatings may have unique properties such as high sensitivity and selectivity.

## 4. Conclusions

Vacuum plasma sprayed titanium oxide coatings possess a porous structure with micro pores and nanosized grains. The main crystal phase of the coatings is rutile with a small amount of anatase. Low-valance titanium cations are found in coating (B). The $Z^*$-planes of both coating (A) and coating (B) show discernible overlapping semicircles corresponding to contributions of grain body and grain boundary. The $C^*$-plane analyses indicate different conductive mechanisms. Plasma sprayed nano-titania coating exhibited unique electric properties, such as adjustable resistance and capacitance. These electric properties are closely associated with the nanophase structure and intergranular component as well as the low-valance titanium cations, which can be controlled with the plasma spraying parameters.

## Acknowledgements

The authors gratefully acknowledge Professor Wang Pingchu for his fruitful discussion and help with the impedance measurements.

## References

1. Huang, A. and Luo, R., Recent development in gas and humidity sensors. *Chemical Sensors*, 1977, **17**(4), 253–263.
2. Azad, A. M., Akbar, S. A., Mhaisalkar, S. G., Birkefeld, L. D. and Goto, K. S., Solid-state gas sensors: a review. *J. Electrochem. Soc.*, 1992, **139**(12), 3690–3704.
3. Tian, J. M., Study on $SnO_2$ gas sensor by complex impedance spectroscopy. *J. Inorg. Mater.*, 1996, **11**(1), 113–118.
4. Birkefeld, L. D., Azad, A. M. and Akbar, S. A., Carbon monoxide and hydrogen detection by anatase modification of titanium oxide. *J. Am. Ceram. Soc.*, 1992, **75**, 2964–2968.
5. Kimura, M., A new method to measure the absolute-humidity independently of the ambient temperature. *Sensors and Actuators*, 1996, **B33**, 156–160.
6. Azad, A. M., Younkman, L. B. and Akbar, S. A., Characterization of $TiO_2$-based materials using immittance spectroscopy. *J. Am. Ceram. Soc.*, 1994, **77**, 481–486.
7. Lin, H. M., Keng, C. H. and Tung, C. Y., Gas-sensing properties of nanocrystalline $TiO_2$. *Nanostruct. Mater.*, 1977, **9**, 747–750.
8. Dong, L. F., Cui, Z. L. and Zhang, Z. K., Gas sensing properties of nano-ZnO prepared by are plasma method. *Nanostruct. Mater.*, 1997, **8**, 815–823.
9. Lavernia, E. J., Kabacoff, L. and Ruhle Davos, M. (chairs), *Thermal Spray Processing of Nano-scale Materials*. Switzerland, 3–8 August 1997.
10. Seitz, M. A., Study of heterogeneous composite materials via lumped parameter/complex plane analysis. *Int. J. Hybrid Microelectron.*, 1980, **3**, 1–7.
11. Huang, J. H., Gao, L., Chen, J. Y. and Yan, D. S., Controlling crystallinity of nano-titania powder prepared by the hydrolysis of titanium alkoxide. *J. Inorg. Mater*, 1996, **11**(1), 51–56.
12. JCPDS, *Powder Diffraction File*, set 21 to 22, Inorganic volume, No. PDIS-22IRB, JCPDS International Center for Diffraction Data, 1601 Park Lane, Swarthmore, PA, 19081, 1983.
13. Wagner, C. D., Riggs, W. M., Davies L. E, Moulder, J. F. and Muilenberg, G. E, *Handbook of X-ray Photoelectron Spectroscopy*. Perkin–Elmer, Eden Prairie, MN, 1979.
14. Zhu, Y. C., Huang, M. H., Chang, C. K. and Ding, C. X., Investigation on structural transform of nano-titania powders during plasma spraying process. *J. Inorg. Mater.*, 1998, **113**(6), 923–926.
15. Herbert, H., Plasma sprayed coating. *Kexue*, 1989, **1**, 25–28.
16. Kingery, W. D., *Introduction to Ceramics*. John Wiley & Sons, Inc.,, New York, 1876 (Chapter 17).
17. Alim, M. A., Admittance-frequency response in zinc oxide varistor ceramics. *J. Am. Ceram. Soc.*, 1989, **72**(1), 28–32.
18. Alim, M. A., Seitz, M. A. and Hirthe, R. W., Complex plane analysis of trapping phenomena in zinc oxide based varistor grain boundaries. *J. Appl. Phys*, 1988, **63**(7), 2337–2345.
19. Wang, R., Li, G., Qu, Z. and Zhen, J., Influence of DSPP $ZrO_2$ on the electrical conductivity PESC-NaSCN complex. *Proceedings of the 9th National Solid State ionics Conference*, 24–27 August 1998, China, pp. 186–190.
20. Zhang, L. D. and Mou, J. M., *Science of Nanostructured Materials*. Science and Technology Press of Liaoning, Liaoning, 1994 (Chapter 2).